PHYSICAL REVIEW C VOLUME 23, NUMBER 1 JANUARY 1981

Interacting boson approximation model of the tungsten isotopes

Philip D. Duval and Bruce R. Barrett
Department of Physics, University of Arizona, Tucson, Arizona 85721
(Received 16 May 1980)

The interacting boson approximation model of Arima and Iachello and co-workers has been used to make a schematic study of the tungsten isotopes. For each isotope of tungsten we determine the values of the five parameters in the interacting boson approximation Hamiltonian which yield the best fit to the experimental energy spectrum. Based on these values, we can extrapolate to isotopes for which no experimental data exist and can make predictions for future experiments. Using the same values of these parameters for each isotope, we can also obtain the $B(E2)$ transition rates, the $\rho(E0)$ values, the quadrupole moments of the first two excited 2^+ states, the two-neutron separation energies, and the isomer and isotope shifts. Where data exist our results, in general, agree very well with experiment, although more experimental information is needed for the isomer and isotope shifts and the quadrupole moments of the excited 2^+ states. The long range goal is to understand the origin of the model parameters in terms of a microscopic theory, such as the nuclear shell model.

[NUCLEAR STRUCTURE Interacting boson approximation model, investigation of the tungsten isotopes, energies, $B(E2)$ transition rates, and other properties. Model parameters as a smooth function of neutron number.]

I. INTRODUCTION

The interacting boson approximation (IBA) model of Arima and Iachello[1,2] has enjoyed continued success in describing the low-lying collective states of several medium and heavy mass nuclei. In this paper we apply the model to the tungsten isotopes ($Z=74$, $82<N<126$). In the IBA, the collective Hamiltonian is written in terms of paired protons and paired neutrons identified as proton bosons and neutron bosons. Each pair can couple to $J=0$ (s boson) or $J=2$ (d boson).

We consider an even-even nucleus with N_π and N_ν proton and neutron pairs, respectively, outside a closed major shell, and treat it as a system of N_π and N_ν interacting proton and neutron bosons. The number of pairs is counted from the nearest closed shell, i.e., we count the number of pairs from the beginning to the middle of a shell and we count the number of hole-pairs from the middle to the end of a shell. For example, in $^{176}_{74}W_{102}$ the proton pairs occupy the 50 to 82 shell so that we have 4 proton boson holes ($N_\pi=4$) and the neutron pairs occupy the 82 to 126 shell so that we have 10 neutron boson particles ($N_\nu=10$).

To obtain the energy spectrum for $^{176}_{74}W_{102}$ we use an appropriate set of parameters in the IBA Hamilitonian and diagonalize this Hamiltonian in the space of the states made from 4 proton s and d bosons and 10 neutron s and d bosons. This is done by the computer code NPBOS developed by Otsuka and Scholten.[2,3] In Sec. II we discuss the nature of the IBA Hamiltonian and in Sec. III present the result of a fit to the known energy spectra of the tungsten isotopes.

Having obtained the wave functions for the energy states from NPBOS, it is then a relatively simple matter to obtain the electromagnetic transition rates. This is done by the computer code NPBEM, also developed by Otsuka and Scholten.[3] In Sec. IV, we present the predictions for the $E0$ and $E2$ transition rates and compare them with experiment. From the $E0$ matrix elements we can extract the isotope and isomer shifts, and from the $E2$ matrix elements we obtain the quadrupole moments. These results are presented in Sec. V, along with the two-neutron separation energies, which are evaluated from the energy spectra calculated by NPBOS. Section VI contains our conclusions.

II. THE INTERACTING BOSON APPROXIMATION

We consider a system of N_π proton bosons and N_ν neutron bosons outside a closed shell and assume that these bosons do not interact with the bosons inside the closed shell (the core bosons). The contribution of the core to the Hamiltonian is then merely a constant term. So we write the Hamiltonian in terms of the valence bosons only,

$$H=H_\pi+H_\nu+V_{\pi\nu}\,, \tag{1}$$

where H_π represents the single-boson energies and boson-boson interactions for the proton bosons, H_ν represents the same for the neutron bosons, and $V_{\pi\nu}$ is the interaction between the

proton and neutron bosons. These energies and interactions can, in principle, be derived from a microscopic theory,[2,4] but in this paper we treat the problem phenomenologically.

In our model Hamiltonian we want to incorporate the essential features of the underlying microscopic picture in fermion space. These features are a strong pairing force between identical particles and a strong quadrupole interaction between nonidentical particles.[1,2]

If two identical nucleons are completely paired (i.e., they have oppositely aligned spins) they form an s boson. They can also align their spins to give $J=2$, forming a d boson. They can, of course, couple to other even values of J (odd values are not allowed because of the Pauli exclusion principle), but for realistic nuclear interactions the pair is either unbound or only weakly bound for $J \geq 4$.[5] So the nature of the IBA is to work in a model space made up of s and d bosons.

With only a pairing force we could write the Hamiltonian as

$$H = \epsilon_{s_\pi} \hat{n}_{s_\pi} + \epsilon_{d_\pi} \hat{n}_{d_\pi} + \epsilon_{s_\nu} \hat{n}_{s_\nu} + \epsilon_{d_\nu} \hat{n}_{d_\nu} , \tag{2}$$

where ϵ_s gives the energy per s boson (i.e., the strength of the fermion interaction forming $J=0$ pairs in the nucleus) and ϵ_d gives the energy per d boson ($J=2$ pairs). The symbol $\hat{}$ above n_{s_π}, etc., indicates that they are operators. But noting that $\hat{n}_{s_\pi} + \hat{n}_{d_\pi} = \hat{N}_\pi$ and $\hat{n}_{s_\nu} + \hat{n}_{d_\nu} = \hat{N}_\nu$, we can write

$$H = \epsilon_{s_\pi} N_\pi + (\epsilon_{d_\pi} - \epsilon_{s_\pi}) \hat{n}_{d_\pi} + \epsilon_{s_\nu} N_\nu + (\epsilon_{d_\nu} - \epsilon_{s_\nu}) \hat{n}_{d_\nu} . \tag{3}$$

Now, $\epsilon_{s_\pi} N_\pi$ and $\epsilon_{s_\nu} N_\nu$ are constants and, for the purpose of calculating relative energy spectra, will not be included in the Hamiltonian. Furthermore, defining $\bar{\epsilon}_\pi \equiv \epsilon_{d_\pi} - \epsilon_{s_\pi}$ and $\bar{\epsilon}_\nu \equiv \epsilon_{d_\nu} - \epsilon_{s_\nu}$, we may now write

$$H = \bar{\epsilon}_\pi \hat{n}_{d_\pi} + \bar{\epsilon}_\nu \hat{n}_{d_\nu} , \tag{4}$$

thereby eliminating the s-boson degrees of freedom.

To include a quadrupole interaction, we add a term of the form $T_\pi \cdot T_\nu$ to the above interaction, where T_π and T_ν are quadrupole operators formed by the coupling of single-boson operators to $J=2$. The most general way to do this is to write

$$T_\rho = \kappa_\rho [(d^\dagger \times s + s^\dagger \times \tilde{d})^{(2)}_\rho + \chi_\rho (d^\dagger \times \tilde{d})^{(2)}_\rho] , \tag{5}$$

where $\rho = \pi$ or ν and s, $s^\dagger$, $\tilde{d}$, and $d^\dagger$ are spherical tensor operators which annihilate and create s and d bosons, respectively.

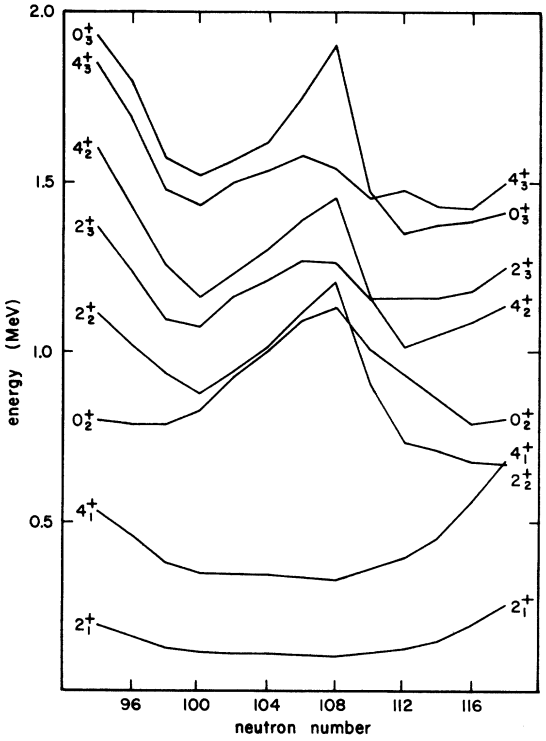

FIG. 1. Calculated energy spectra of the tungsten isotopes showing the low-lying 0^+, 2^+, and 4^+ states, with respect to the 0^+ ground state.

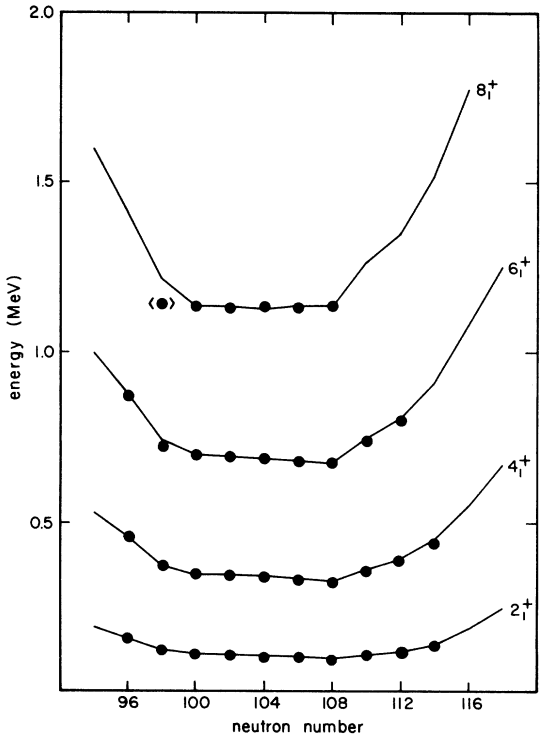

FIG. 2. Comparison between calculated and experimental energy levels of the tungsten isotopes in the *ground state band*. The experimental points are from Refs. 8 and 10 and are ordered in increasing energy as 2_1^+, 4_1^+, 6_1^+, and 8_1^+.

If we define $\kappa = \kappa_\pi \kappa_\nu$ and

$$Q_\rho = (d^\dagger \times s + s^\dagger \times \tilde{d})^{(2)}_\rho + \chi_\rho (d^\dagger \times \tilde{d})^{(2)}_\rho, \quad \rho = \pi, \nu \tag{6}$$

the Hamiltonian can be written as

$$H = \bar{\epsilon}_\pi \hat{n}_{d_\pi} + \bar{\epsilon}_\nu \hat{n}_{d_\nu} + \kappa Q_\pi \cdot Q_\nu \, . \tag{7}$$

We also include a residual proton-proton interaction and neutron-neutron interaction in our Hamiltonian. The residual interactions used conserve the number of d bosons, corresponding to the conservation of seniority in the underlying fermion space. The form for these residual interactions is[1]

$$\begin{aligned} \tilde{V}_{\rho\rho} = & \sum_{L=0,2,4} \tfrac{1}{2}(2L+1)^{1/2} \tilde{C}^\rho_L [(d^\dagger_\rho \times d^\dagger_\rho)^{(L)} \cdot (\tilde{d}_\rho \times \tilde{d}_\rho)^{(L)}]^{(0)} \\ & + \tfrac{1}{2} u^\rho_0 [(s^\dagger_\rho \times s^\dagger_\rho)^{(0)} \cdot (s_\rho \times s_\rho)^{(0)}]^{(0)} \\ & + u^\rho_2 [(d^\dagger_\rho \times s^\dagger_\rho)^{(2)} \cdot (\tilde{d}_\rho \times s_\rho)^{(2)}]^{(0)}, \quad \rho = \pi, \nu \, . \end{aligned} \tag{8}$$

As in the case of the single-boson energies, we can eliminate the s boson degrees of freedom from this interaction. The details are worked out in Ref. 1. The result is that we can rewrite the above equation as

$$\tilde{V}_{\rho\rho} = \tfrac{1}{2} u^\rho_0 N_\rho (N_\rho - 1) + \epsilon'_\rho \hat{n}_{d_\rho} + V_{\rho\rho} \, , \tag{9}$$

where

$$\begin{aligned} V_{\rho\rho} = & \sum_{L=0,2,4} \tfrac{1}{2}(2L+1)^{1/2} C^\rho_L \\ & \times [(d^\dagger_\rho \times d^\dagger_\rho)^{(L)} \cdot (\tilde{d}_\rho \times \tilde{d}_\rho)^{(L)}]^{(0)} \, , \end{aligned} \tag{10}$$

$$\epsilon'_\rho = (u^\rho_2/\sqrt{5} - u^\rho_0)(N_\rho - 1) \, , \tag{11}$$

$$C^\rho_0 = \tilde{C}^\rho_0 + u^\rho_0 \, , \tag{12}$$

and

$$C^\rho_2 = \tilde{C}^\rho_2 - u^\rho_2/\sqrt{5}, \quad \rho = \pi, \nu \, . \tag{13}$$

The first term on the right-hand side of Eq. (9) is a constant, and, again is not included in our model Hamiltonian.

Finally, we include a Majorana term. The Majorana term fixes the location of states with mixed proton-neutron symmetry with respect to the totally symmetric states. This term should

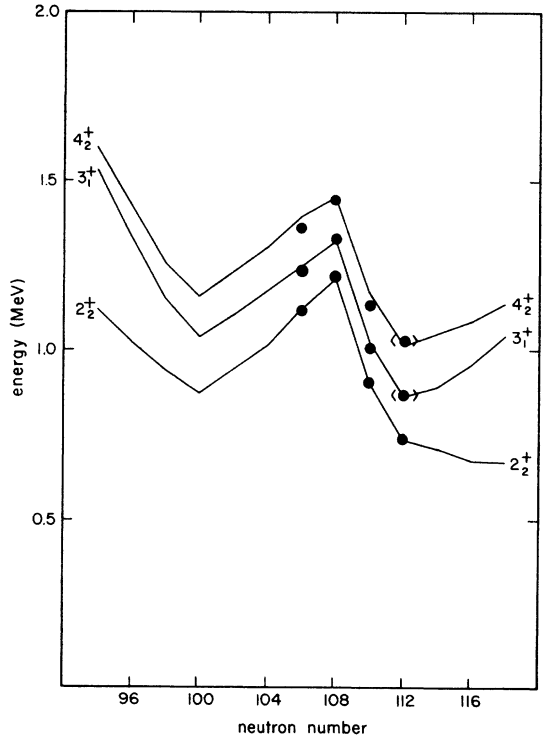

FIG. 3. Comparison between calculated and experimental energy levels of the tungsten isotopes in the *quasi-γ band.* The experimental points are from Refs. 8 and 9 and are ordered in increasing energy as 2^+_2, 3^+_1, and 4^+_2. Bracketed states are listed as questionable.

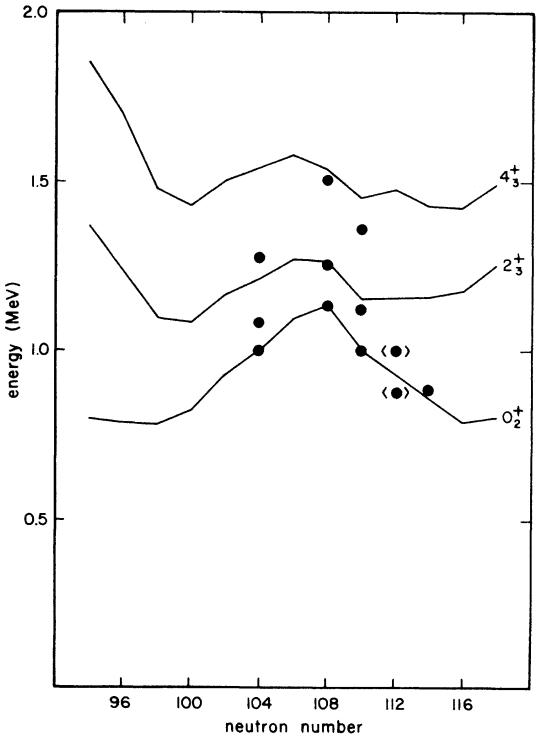

FIG. 4. Comparison between calculated and experimental energy levels of the tungsten isotopes in the *quasi-β band.* The experimental points are from Ref. 8 and are ordered in increasing energy as 0^+_2, 2^+_3, and 4^+_3. Bracketed states are questionable.

include those terms which are antisymmetric under the interchange of proton and neutron bosons. It is given in the following form[2]:

$$M_{\pi\nu} = \xi_2 (s_\nu^\dagger \times d_\pi^\dagger - d_\nu^\dagger \times s_\pi^\dagger)^{(2)} \cdot (s_\nu \times \tilde{d}_\pi - \tilde{d}_\nu \times s_\pi)^{(2)} + \sum_{\kappa=1,3} \xi_\kappa (d_\nu^\dagger \times d_\pi^\dagger)^{(\kappa)} \cdot (\tilde{d}_\nu \times \tilde{d}_\pi)^{(\kappa)} . \quad (14)$$

Collecting all of the previous terms, we obtain for the Hamiltonian

$$H = \epsilon_\pi \hat{n}_{d_\pi} + \epsilon_\nu \hat{n}_{d_\nu} + \kappa Q_\pi \cdot Q_\nu + V_{\pi\pi} + V_{\nu\nu} + M_{\pi\nu} , \quad (15)$$

where $\epsilon_\pi = \bar{\epsilon}_\pi + \epsilon'_\pi$ and $\epsilon_\nu = \bar{\epsilon}_\nu + \epsilon'_\nu$ are the renormalized single-boson energies.

The structure of the energy spectra is determined mainly by the first three terms on the right-hand side of Eq. (15) (the pairing plus quadrupole terms), while the remaining terms have minor, but non-negligible contributions. This is borne out by our calculations for the tungsten isotopes. We expect the importance of the $V_{\pi\pi}$ term (or the $V_{\nu\nu}$ term) to be manifest when there are many more proton bosons than neutron bosons (or vice-versa). We also assume that those parameters in the Hamiltonian labeled with a π depend only on proton number and those labeled with a ν depend only on neutron number. Those left unsubscripted may depend on both proton and neutron number.

III. THE ENERGY SPECTRA

We now apply the model described in the previous section to the calculation of the energy spectra of the tungsten isotopes ($Z=74$, $N_\pi=4$ and $82<N<126$, $0<N_\nu\leq 11$). To reduce the number of free parameters, the following simplifications are made.

First, we set $\epsilon_\pi = \epsilon_\nu \equiv \epsilon$, which is the usual assumption.[2,6,7] This might seem an oversimplification, especially since the proton bosons and neutron bosons are in different shells. However, calculations using this assumption have led to reasonable results, not only for tungsten, but also for other nuclides.

Second, we include only the C_0 and C_2 terms in the $V_{\nu\nu}$ interaction and do not include at all the $V_{\pi\pi}$ interaction since, for most of the region fitted, $N_\nu > N_\pi$ and we do not expect the $V_{\pi\pi}$ term to be very important.

Last, in the Majorana term we set $\xi_2 = 0.04$ MeV and $\xi_1 = \xi_3 = -0.02$ MeV for the entire isotopic chain. The Majorana term is used primarily to

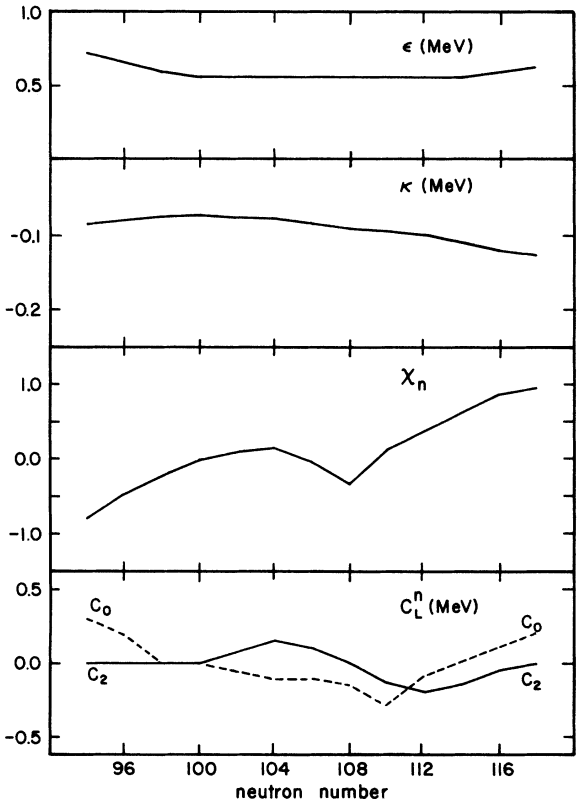

FIG. 5. The parameter set used for the tungsten isotopes. The value used for χ_π was −1.6.

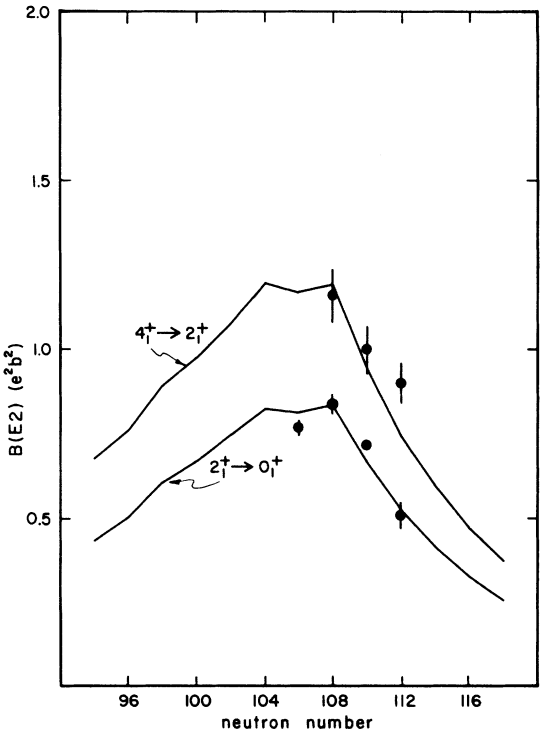

FIG. 6. Comparison between calculated and experimental $B(E2)$ values for the $2_1^+ \rightarrow 0_1^+$ and $4_1^+ \rightarrow 2_1^+$ transitions. The experimental points are from Ref. 12.

push up in energy those states with large antisymmetric parts. Since the low-lying collective states are largely symmetric, we then expect the influence of the Majorana term on these states to be minimal.[2]

With these simplifications, the Hamiltonian used in our fit to the tungsten isotopes becomes

$$H = \epsilon \hat{n}_d + \kappa Q_\pi \cdot Q_\nu + V_{\nu\nu} + M_{\pi\nu} , \qquad (16)$$

where $\hat{n}_d = \hat{n}_{d_\pi} + \hat{n}_{d_\nu}$, and we now have only six free parameters: ϵ, κ, χ_π, χ_ν, C_0, and C_2. After one isotope is fitted, we establish χ_π, which is kept constant for the remaining isotope fits, so that we use only five free parameters thereafter. We again note that the main features of the energy spectra are determined by the first two terms in the above Hamiltonian, i.e., by the parameters ϵ, κ, χ_π, and χ_ν.

The experimentally determined energy levels for the even-even tungsten isotopes span the range in neutron number from $N = 96$ to $N = 114$. We can make predictions beyond this region by a smooth extrapolation of the above parameters.

In Fig. 1, we present the results of our calculation of the energy levels for the isotopic chain $^{168}_{74}W_{94}$ to $^{192}_{74}W_{118}$, and in Figs. 2–4 we give a detailed comparison with the experimental data according to the quasi-ground state rotational band and the quasi-γ and β vibrational bands. Figure 5 contains graphs of the parameters used. A list of these parameters is available upon request.

Perhaps the most striking feature of the energy spectra is the sharp rise in the γ and β bands at neutron number $N = 108$, which may be due to a subshell closure in the $i_{13/2}$ Nilsson level and/or a reversal in the deformation. This is supported by such effects as a large change in the two neutron separation energy after $N = 108$. This same rise also occurs in the γ band of the neighboring osmium isotopes ($Z = 76$). Fitting this has led to a dip in the value of χ_ν at $N = 108$. Note that the IBA predicts a dramatic increase in the 0_3^+ state at this neutron number. This state is, as yet, unknown experimentally for $^{182}_{74}W_{108}$.

Another interesting feature is a relatively sharp increase in the ground state band at $N = 96$. Once again, this same feature shows up in the osmium data. When the ground state band is fitted for $^{170}_{74}W_{96}$, the IBA predicts even larger increases in the higher energy levels of the γ and β bands.

In, general, the agreement with experiment for the ground-state-band and γ-band energy levels is quite good. The agreement with the β-band

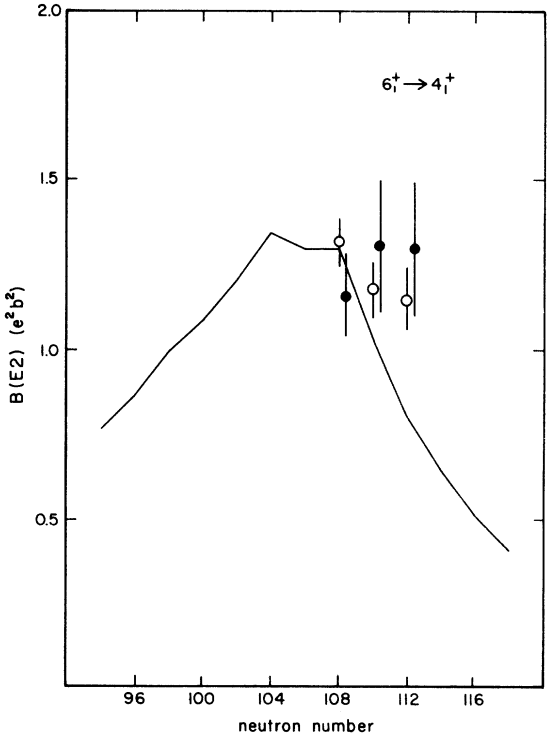

FIG. 7. Comparison between calculated and experimental $B(E2)$ values for the $6_1^+ \rightarrow 4_1^+$ transition. The solid circles are from Ref. 12. The open circles are from Ref. 18.

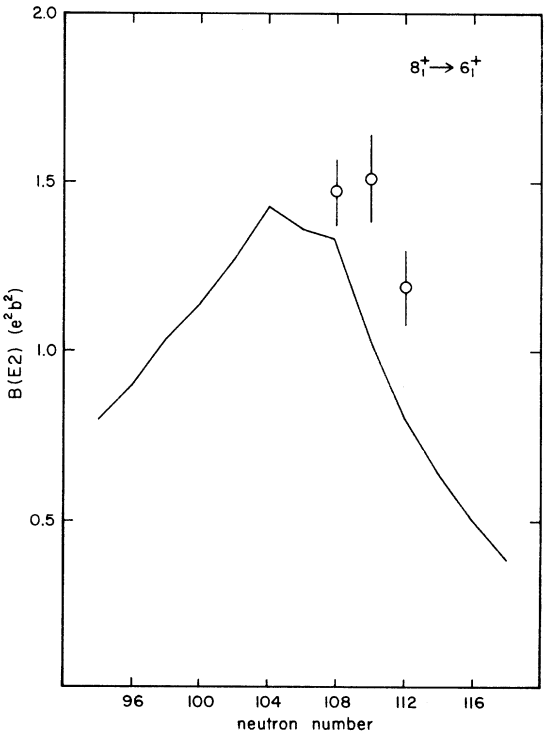

FIG. 8. Comparison between calculated and experimental $B(E2)$ values for the $8_1^+ \rightarrow 6_1^+$ transition. The experimental points are from Ref. 18.

energies, however, is not as successful, notably in $^{186}_{74}W_{112}$ and $^{178}_{74}W_{104}$. The IBA predicts the β-bands energy levels for these two isotopes to be much farther apart than experiment seems to indicate. In the case of $^{186}_{74}W_{112}$, however, one should note that the experimental β-band energies are listed as questionable.

IV. ELECTROMAGNETIC TRANSITION RATES

Having obtained the wave functions for the energy states in the tungsten isotopes by fitting to the experimental energy levels, we can determine the electromagnetic transition rates between these states. The most general single-boson transition operator of angular momentum l can be written as[1]

$$T^{(l)} = T_\pi^{(l)} + T_\nu^{(l)} , \tag{17}$$

where

$$T_\rho^{(l)} = \alpha_{2\rho}\delta_{l2}(d^\dagger \times s + s^\dagger \times \tilde{d})_\rho^{(2)} + \beta_{l\rho}(d^\dagger \times \tilde{d})_\rho^{(l)} + \gamma_{0\rho}\delta_{l0}(s^\dagger \times s)_\rho^{(0)}, \quad \rho = \pi, \nu , \tag{18}$$

and $\alpha_{2\rho}$, $\beta_{l\rho}$ ($l = 0, 1, 2, 3, 4$), and $\gamma_{0\rho}$ are new parameters. In this section we will examine the $T^{(E2)}$ and $T^{(E0)}$ operators and present our results for the reduced transition rates, $B(E2)$ and $\rho(E0)$, for the tungsten isotopes.

A. $E2$ transitions

Using $l = 2$ in Eqs. (17) and (18) we find the $E2$ transition operator to be given by

$$T^{(E2)} = \alpha_{2\pi}(d^\dagger \times s + s^\dagger \times \tilde{d})_\pi^{(2)} + \beta_{2\pi}(d^\dagger \times \tilde{d})_\pi^{(2)} + \alpha_{2\nu}(d^\dagger \times s + s \times \tilde{d})_\nu^{(2)} + \beta_{2\nu}(d^\dagger \times \tilde{d})_\nu^{(2)}$$

which may be written as

$$T^{(E2)} = e_\pi[(d^\dagger \times s + s^\dagger \times \tilde{d})_\pi^{(2)} + \chi_\pi(d^\dagger \times \tilde{d})_\pi^{(2)}] + e_\nu[(d^\dagger \times s + s^\dagger \times \tilde{d})_\nu^{(2)} + \chi_\nu(d^\dagger \times \tilde{d})_\nu^{(2)}] = e_\pi Q_\pi + e_\nu Q_\nu . \tag{19}$$

In principle, the parameters χ_π and χ_ν may be different from those used in the quadrupole operators in the Hamiltonian (Eq. 5), however, we have taken them to be the same in our calculations so as to reduce the number of free parameters. This also seems a natural choice. The paramet-

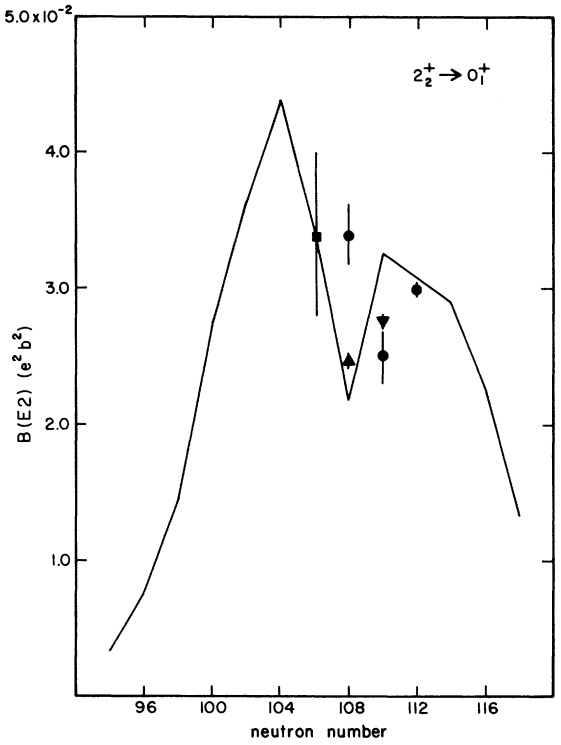

FIG. 9. Comparison between calculated and experimental $B(E2)$ values for the $2_2^+ \rightarrow 0_1^+$ transition. The circles are from Ref. 12, the squares from Ref. 15, the delta symbols from Ref. 13, and the inverted deltas from Ref. 16.

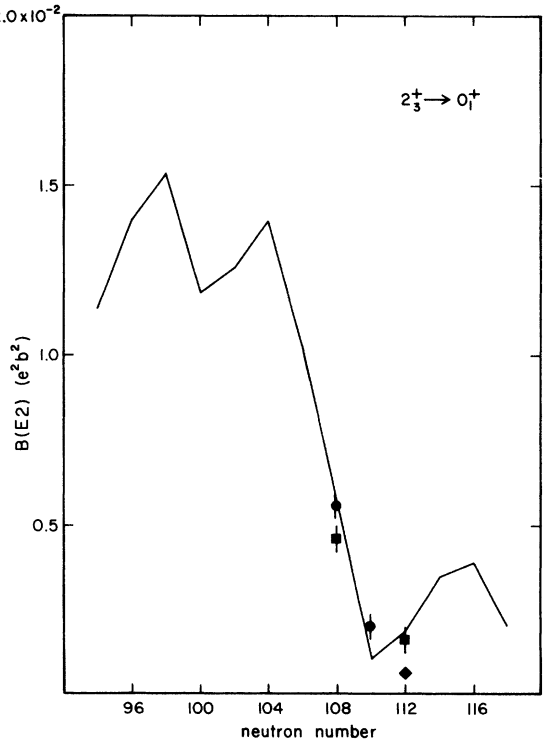

FIG. 10. Comparison between calculated and experimental $B(E2)$ values for the $2_3^+ \rightarrow 0_1^+$ transition. The circles are from Ref. 12, the squares from Ref. 15, and the diamonds from Ref. 14.

ers e_π and e_ν have units of eb and indicate the proton-boson and neutron-boson effective charges. Again recalling Eq. (5), we might expect e_π and e_ν to have the same dependence on proton number and neutron number as do κ_π and κ_ν, however, as an even further simplification, we use $e_\pi = e_\nu$ equals a constant for all nuclei. The value of the constant is determined by fitting one of the experimentally known transition rates. Using $e_\pi = e_\nu = 0.126$ eb (determined by fitting the $2_1^+ \to 0_1^+$ transition in $^{182}_{74}W_{108}$), we obtain the results shown in the following figures. We present the results using the more conventional reduced transition rates, i.e., the $B(E2)$ values, given by[11]

$$B(E2; i \to f) = \frac{1}{2J_i + 1} \left| \langle J_f \| T^{(E2)} \| J_i \rangle \right|^2 . \quad (20)$$

Figures 6–11 give the absolute $B(E2)$ values for the $2_1^+ \to 0_1^+$, $4_1^+ \to 2_1^+$, $6_1^+ \to 4_1^+$, $8_1^+ \to 6_1^+$, $2_2^+ \to 0_1^+$, $2_3^+ \to 0_1^+$, and $2_2^+ \to 2_1^+$ transitions, and Figs. 12–14 show the branching ratios $B(E2; 2_2^+ \to 0_1^+)/B(E2; 2_2^+ \to 2_1^+)$, $B(E2; 3_1^+ \to 2_1^+)/B(E2; 3_1^+ \to 4_1^+)$, and $B(E2; 2_2^+ \to 4_1^+)/B(E2; 2_2^+ \to 2_1^+)$. These are compared with several sets of experimental data,[12–18] the major source of data being Ref. 12.

Our agreement with the available data is generally quite good. It should be noted that *no attempt* was made to fit any of the $B(E2)$ values while determining the parameters in the Hamiltonian.

B. $E0$ transitions

The $E0$ transition operator is found by setting $l = 0$ in Eqs. (17) and (18), giving

$$T^{(E0)} = \beta_{0_\pi}(d^\dagger \times \tilde{d})_\pi^{(0)} + \gamma_{0_\pi}(s^\dagger \times s)^{(0)} + \beta_{0_\nu}(d^\dagger \times \tilde{d})_\nu^{(0)} + \gamma_{0_\nu}(s^\dagger \times s)_\nu^{(0)} . \quad (21)$$

Now, the s and d boson number operators are written in terms of the above creation and annihilation operators as follows: $\hat{n}_{d_\rho} = \sqrt{5}\,(d^\dagger \times \tilde{d})_\rho^{(0)}$, $\hat{n}_{s_\rho} = (s^\dagger \times s)_\rho^{(0)}$ $(\rho = \pi, \nu)$. Therefore, recalling that $\hat{N}_\rho = \hat{n}_{d_\rho} + \hat{n}_{s_\rho}$ we may write

$$T^{(E0)} = \tilde{\beta}_{0_\pi}\hat{n}_{d_\pi} + \gamma_{0_\pi}N_\pi + \tilde{\beta}_{0_\nu}\hat{n}_{d_\nu} + \gamma_{0_\nu}N_\nu , \quad (22)$$

where

$$\tilde{\beta}_{0_\rho} = (\beta_{0_\rho}/\sqrt{5}) - \gamma_{0_\rho}, \quad \rho = \pi, \nu . \quad (23)$$

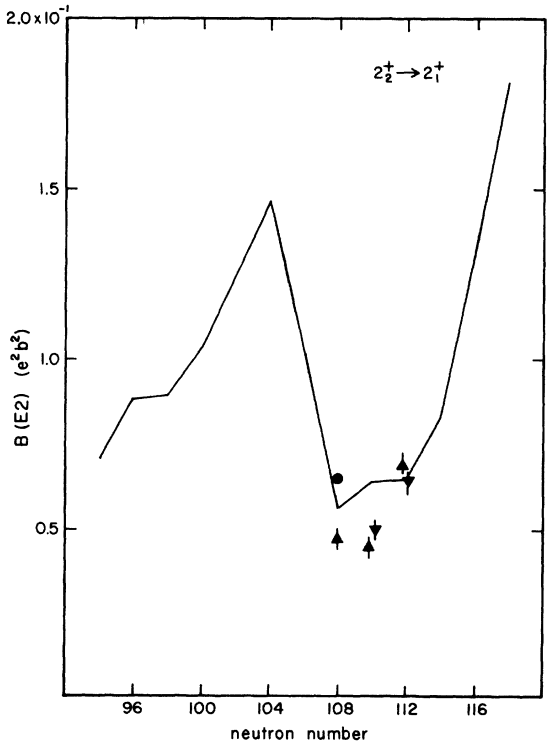

FIG. 11. Comparison between calculated and experimental $B(E2)$ values for the $2_2^+ \to 2_1^+$ transition. The circles are from Ref. 12, the delta symbols from Ref. 13, and the inverted deltas from Ref. 16.

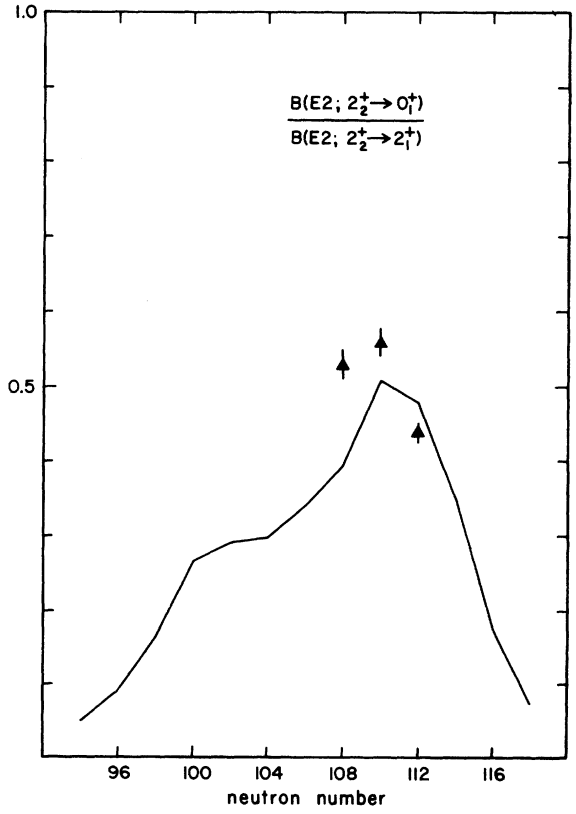

FIG. 12. Comparison between calculated and experimental $B(E2; 2_2^+ \to 0_1^+)/B(E2; 2_2^+ \to 2_1^+)$ ratios. The experimental points are from Ref. 13.

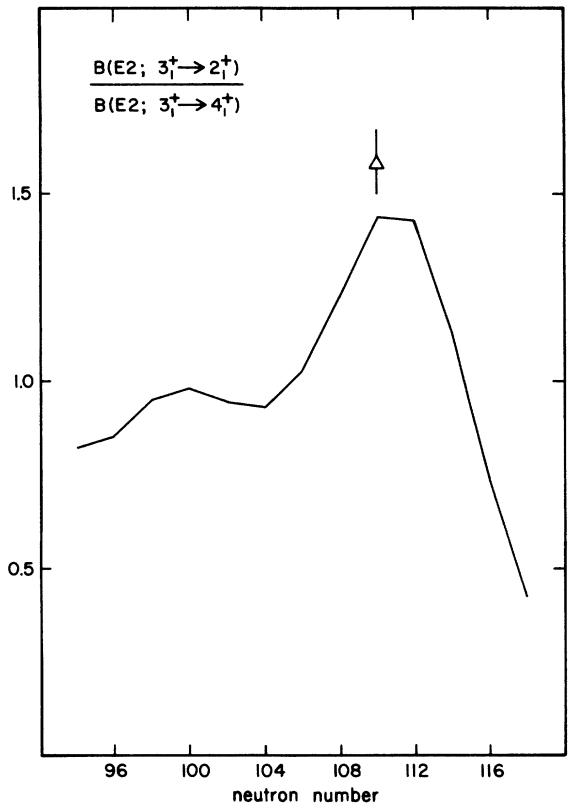

FIG. 13. Comparison between calculated and experimental $B(E2; 3_1^+ \rightarrow 2_1^+)/B(E2; 3_1^+ \rightarrow 4_1^+)$ ratios. The experimental point is from Ref. 17.

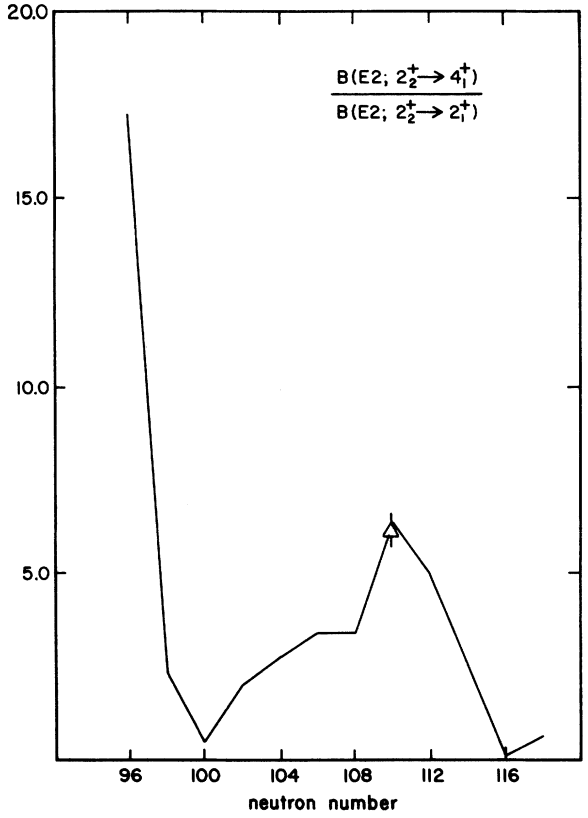

FIG. 14. Comparison between calculated and experimental $B(E2; 2_2^+ \rightarrow 4_1^+)/B(E2; 2_2^+ \rightarrow 2_1^+)$ ratios. The experimental point is from Ref. 17.

The terms $\gamma_{0_\pi} N_\pi$ and $\gamma_{0_\nu} N_\nu$ are constant and do not give rise to transitions. Furthermore, we choose the parameters $\bar{\beta}_{0_\rho}$ and γ_{0_ρ} to have units of fm^2, since, in configuration space, that part of the $E0$ operator which gives rise to transitions is proportional to r^2.[11] The conventional $\rho(E0)$ transition matrix elements are then written in terms of the above operators as

$$\rho(E0_i J_i \rightarrow J_f) = \frac{Z}{R_0^2} \left(\bar{\beta}_{0_\pi} \langle J_f | \hat{n}_{d_\pi} | J_i \rangle + \bar{\beta}_{0_\nu} \langle J_f | \hat{n}_{d_\nu} | J_i \rangle \right), \tag{24}$$

where $R_0 = r_0 A^{1/3}$ is the radius of the nucleus, and $\rho(E0)$ is a dimensionless quantity. In Table I, we compare several theoretical versus experimental $\rho(E0)$ values. We use $\bar{\beta}_{0_\pi} = 0.075$ fm^2 and $\bar{\beta}_{0_\nu} = -0.045$ fm^2, which were obtained entirely from fitting the isotope and isomer shifts (see Sec. V). There is good agreement with experiment only for the $2_3^+ \rightarrow 2_1^+$ transition in ^{182}W. However, the other experimental values do have large uncertainties. Other theoretical $\rho(E0)$ values are available upon request.

V. OTHER PROPERTIES

In this section we present the results for the calculated quadrupole moments, isotope shifts, isomer shifts, and two-neutron separation energies.

A. Quadrupole moments

The $E2$ transition operators is, in fact, a quadrupole operator. The definition of the quadrupole moment for a nucleus in a state characterized by angular momentum J is

$$Q_J = \left(\frac{16\pi}{5}\right)^{1/2} \begin{pmatrix} J & 2 & J \\ -J & 0 & J \end{pmatrix} \langle J \| T^{(E2)} \| J \rangle . \tag{25}$$

TABLE I. $\rho(E0)$ transition matrix elements. The data are from Ref. 19.

$\rho(E0; i \rightarrow f)$	Experiment	Theory
^{182}W: $2_3^+ \rightarrow 2_1^+$	$4.0 \pm (0.6) \times 10^{-2}$	5.95×10^{-2}
	$4.9 \pm (0.5) \times 10^{-2}$	
^{184}W: $2_2^+ \rightarrow 2_1^+$	$2.9^{+1.5}_{-2.9} \times 10^{-2}$	0.252×10^{-2}
	$1.6^{+4.0}_{-1.2} \times 10^{-2}$	

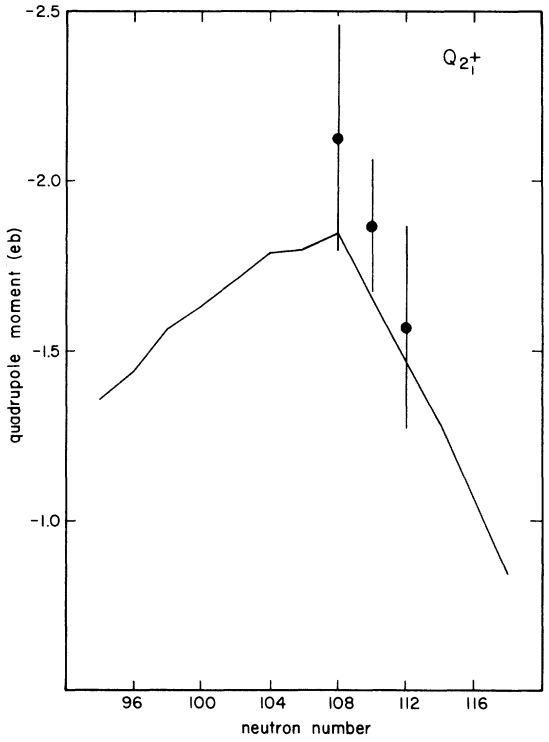

FIG. 15. Comparison between calculated and experimental quadrupole moments for the 2_1^+ state. The experimental points are from Ref. 21.

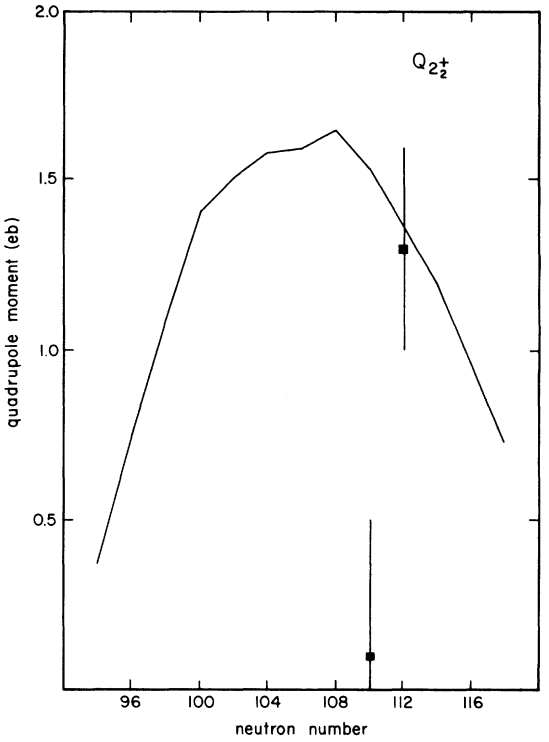

FIG. 16. Comparison between calculated and experimental quadrupole moments for the 2_2^+ state. The experimental points are from Ref. 21.

Using the IBA wave functions and $E2$ transition operator given by Eq. (19), we obtain the results shown in Figs. 15 and 16 for $J=2_1^+$ and $J=2_2^+$. Note that the parameters e_π and e_ν in the $T^{(E2)}$ operator have already been determined from fitting the $B(E2)$ data ($e_\pi = e_\nu = 0.126$ eb) and as before, χ_ν and χ_π are the same numbers used in the Hamiltonian [Eq. (15)], so that we fit *no* new free parameters in determining the quadrupole moments. The IBA predicts the correct sign in both of the above cases, and the agreement with experiment is very good for $Q_{2_1^+}$. But, in the case of $Q_{2_2^+}$, the IBA value differs dramatically from the recently determined experimental number for $^{184}_{74}W_{110}$.[21] Experiment indicates a sharp decrease in $Q_{2_2^+}$ for this isotope, which is not predicted by the IBA. This decrease is, however, predicted by the pairing-plus-quadrupole model of Kumar and Baranger,[22] but for other properties associated with the 2_2^+ state (i.e., energy and $E2$ transitions), the IBA agrees much better with experiment. For completeness, we, at this point, present a comparison between the IBA, the model of Kumar and Baranger, and experiment, shown in Table II.

B. Isomer shifts and isotope shifts

In Sec. IV, we noted that the $E0$ transition operator is proportional to r^2. In fact, by our previous choice of units for $\tilde{\beta}_{0_\rho}$ and γ_{0_ρ} in Eq. (22), the expectation value of the $T^{(E0)}$ operator is equal to that of the $\hat{r}^2$ operator, except that we must add a constant term to represent the contribution of the closed shells. That is,

$$\langle r^2 \rangle = \langle r^2 \rangle^{(C)} + \langle T^{(E0)} \rangle \,, \tag{26}$$

where $T^{(E0)}$ is given by Eq. (22) and $\langle r^2 \rangle^{(C)}$ represents the core contribution. Therefore, the isomer shift, which is the difference between the mean square radius $\langle r^2 \rangle$ of the 2_1^+ state and the ground state of a given nucleus, is given by

$$\begin{aligned} \delta\langle r^2 \rangle &= \langle 2_1^+ | r^2 | 2_1^+ \rangle - \langle 0_1^+ | r^2 | 0_1^+ \rangle \\ &= \tilde{\beta}_{0_\pi} (\langle 2_1^+ | \hat{n}_{d_\pi} | 2_1^+ \rangle - \langle 0_1^+ | \hat{n}_{d_\pi} | 0_1^+ \rangle) \\ &\quad + \tilde{\beta}_{0_\nu} (\langle 2_1^+ | \hat{n}_{d_\nu} | 2_1^+ \rangle - \langle 0_1^+ | \hat{n}_{d_\nu} | 0_1^+ \rangle) \,, \end{aligned} \tag{27}$$

and the isotope shift, which is the difference in $\langle r^2 \rangle$ between two neighboring isotopes in their ground states, is given by

TABLE II. Comparison of IBA, K-B, and experiment for $W_{108,110,112}$.

Energy level (MeV)	IBA 108	IBA 110	IBA 112	K-B 108	K-B 110	K-B 112	Exp.[a] 108	Exp.[a] 110	Exp.[a] 112
0_2^+	1.133	1.002	0.933	0.788	0.666	0.573	1.136	1.002	(0.882)
2_1^+	0.100	0.111	0.122	0.104	0.122	0.139	0.100	0.111	0.122
2_2^+	1.21	0.904	0.733	0.936	0.760	0.602	1.22	0.903	0.738
2_3^+	1.26	1.15	1.156	1.063	0.898	0.745	1.26	1.12	(1.006)
3_1^+	1.32	1.022	0.862	1.231	1.060	0.885	1.33	1.006	(0.862)
4_1^+	0.328	0.364	0.394	0.314	0.350	0.380	0.329	0.364	0.396
$B(E2;\ i-f)$ (e^2b^2)									
$2_1^+ \rightarrow 0_1^+$	0.84	0.670	0.525	0.804	0.749	0.700	0.84[b]	0.72[b]	0.51[b]
$2_2^+ \rightarrow 0_1^+$	0.022	0.033	0.031	0.0054	0.017	0.031	0.034[b]	0.0252[c]	0.03[c]
							0.0248[c]	0.0276[f]	
$2_3^+ \rightarrow 0_1^+$	0.0057	0.0011	0.0018	0.0346	0.027	0.0166	0.0056[c]	0.002[e]	0.0016[e]
									0.0006[d]
$2_2^+ \rightarrow 2_1^+$	0.056	0.0641	0.0644	0.104	0.176	0.302	0.065[b]	0.05[f]	0.064[f]
							0.047[c]		
$4_1^+ \rightarrow 2_1^+$	1.19	0.949	0.746	1.205	1.15	1.096	1.16[b]	1.03[b]	0.905[b]
$2_3^+ \rightarrow 2_1^+$	0.0022	0.0014	0.0024	0.016	0.007	0.002	0.0057[c]		
Q $(e\,b)$									
$Q_{2_1^+}$	−1.85	−1.65	−1.46	−1.795	−1.699	−1.409	−2.13[g]	−1.87[g]	−1.57[g]
$Q_{2_2^+}$	1.65	1.53	1.37	0.137	0.736	1.053		0.1[h]	1.3[h]

[a] See Ref. 8.
[b] See Ref. 12.
[c] See Ref. 13.
[d] See Ref. 14.
[e] See Ref. 15.
[f] See Ref. 16.
[g] See Ref. 20.
[h] See Ref. 21.

$$\Delta\langle r^2\rangle = \langle 0_1^+ | r^2 | 0_1^+\rangle_A - \langle 0_1^+ | r^2 | 0_1^+\rangle_{A+2}$$

$$= \tilde{\beta}_{0_\pi}(\langle 0_1^+ | \hat{n}_{d_\pi} | 0_1^+\rangle_{N_\nu'} - \langle 0_1^+ | \hat{n}_{d_\pi} | 0_1^+\rangle_{N_\nu'+1})$$

$$+ \tilde{\beta}_{0_\nu}(\langle 0_1^+ | \hat{n}_{d_\nu} | 0_1^+\rangle_{N_\nu'} - \langle 0_1^+ | \hat{n}_{d_\nu} | 0_1^+\rangle_{N_\nu'+1}) - \gamma_{0_\nu}. \quad (28)$$

We put primes on N_π and N_ν to emphasize that they are to represent, in this case, the number of boson *particles* throughout the entire shell.

Table III shows theoretical versus experimental isomer and isotope shifts. The values of the parameters were determined to be $\tilde{\beta}_{0_\pi} = 0.075$ fm^2, $\tilde{\beta}_{0_\nu} = 0.045$ fm^2, and $\gamma_{0_\nu} = -0.117$ fm^2 by fitting to $\delta\langle r^2\rangle = 0.16 \times 10^{-3}$ fm^2 for $^{184}_{74}W_{110}$,[23] and $\Delta\langle r^2\rangle = 0.120$ fm^2 and 0.092 fm^2 for the isotope shifts $^{182}_{74}W_{108} - ^{184}_{74}W_{110}$ and $^{184}_{74}W_{110} - ^{186}_{74}W_{112}$, respectively.[24] These same values were used in determining the $\rho(E0)$ transition rates in Sec. IV.

The agreement with the remaining experimental points is not very good, although the IBA does predict the experimentally observed sign change in the isomer shift for $^{184}_{74}W_{108}$. It should be noted that the uncertainties in the isomer shift data are roughly an order of magnitude.

Clearly more experimental results on the isomer and isotope shifts for the tungsten isotopes would be very useful to compare with the predictions possible using the IBA.

C. Two-neutron separation energy

The binding energy E_B of a nucleus is given by the negative of its ground-state (g.s.) energy.

TABLE III. Isomer shift and isotope shift. The theoretical points marked with an asterisk were fitted to the data. The uncertainties of the experimental data are roughly an order of magnitude.

Isomer shifts	Experimental	Theory
^{182}W	-0.2×10^{-3} fm^2 [a]	-1.3×10^{-3} fm^2
	-0.37×10^{-3} [b]	
	0.0×10^{-3} [b]	
^{184}W	0.16×10^{-3} [a]	0.16×10^{-3}*
	0.12×10^{-3} [b]	
	0.0×10^{-3} [b]	
^{186}W	0.14×10^{-3} [a]	2.1×10^{-3}
	0.12×10^{-3} [b]	
	-0.49×10^{-3} [b]	
Isotope shifts		
^{180}W-^{182}W	0.074 fm^2 [d]	0.126 fm^2
^{182}W-^{184}W	0.120 [c]	0.120*
^{184}W-^{186}W	0.092 [c]	0.092*

[a] See Ref. 23.
[b] See Ref. 26.
[c] See Ref. 24.
[d] Ratio given in Ref. 25 and absolute numbers of Ref. 24.

This energy is not just the eigenvalue of the 0_1^+ state, since we are looking for an absolute number. We must recall all of the unused constant terms in the Hamiltonian described in Sec. II. These give

$$E_{\text{g.s.}} = -E_B = E_{\text{core}} + \epsilon_{s_\nu} N'_\nu + \epsilon_{s_\pi} N'_\pi + \tfrac{1}{2} u_0^\nu N'_\nu(N'_\nu - 1) + \tfrac{1}{2} u_0^\pi N'_\pi(N'_\pi - 1) + E_{B_{\text{def}}}, \quad (29)$$

where E_{core} is the energy of the closed shells and E_{def} is the deformation energy (i.e., the 0_1^+ eigenvalue using the IBA Hamiltonian). The primes on N_π and N_ν again emphasize that they are to represent boson *particles*.

For constant proton number, the binding energy can thus be written as

$$E_B = A + BN'_\nu + \tfrac{1}{2} CN'_\nu(N'_\nu - 1) + E_{B_{\text{def}}}, \quad (30)$$

where A, B, and C are constants and $E_{B_{\text{def}}} = -E_{\text{def}}$.

Instead of the actual binding energy we will examine the two-neutron separation energy. This is the energy required to remove two neutrons (one neutron boson) from a given isotope and is given by

$$S_{2n}(N'_\nu) = E_B(N'_\nu) - E_B(N'_\nu - 1) = B + C(N'_\nu - 1) + \Delta E_{B_{\text{def}}}, \quad (31)$$

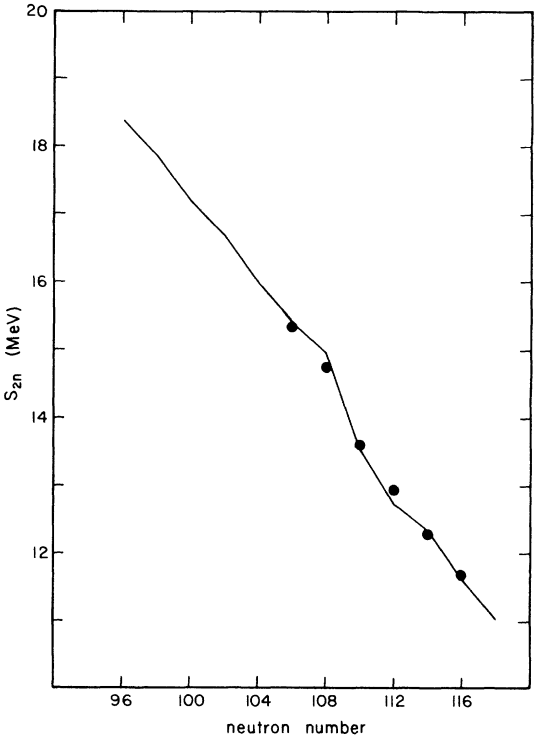

FIG. 17. Comparison between calculated and experimental two-neutron separation energies, S_{2n}. The experimental points are from Ref. 10.

where $\Delta E_{B_{\text{def}}} = E_{B_{\text{def}}}(N'_\nu) - E_{B_{\text{def}}}(N'_\nu - 1)$, with the values $B = 22.05$ MeV and $C = -0.63$ MeV [determined by fitting Eq. (31) to the available experimental data[10]] we obtain the results shown in Fig. 17 for the tungsten isotopes. The agreement with experiment is quite good.

VI. CONCLUDING REMARKS

In this paper we have presented the results of the calculations of various properties of the tungsten isotopes using the interacting boson approximation model of Arima and Iachello. The agreement with experiment is generally quite good, particularly where the energy levels and $E2$ transitions are concerned. Where a comparison can be made, our results for the energy levels and $E2$ transitions are in better agreement with experiment than the earlier calculations of Kumar and Baranger. We have also made a large number of theoretical predictions where data were unavailable. It would be worthwhile for experimentalists to perform further investigations for the tungstens in order to compare them with the theoretical predictions. This is particularly true for the isomer and isotope shifts and the $\rho(E0)$ values, and for the quadrupole moment of the second 2^+ state, which we predict to have a trend

with changing neutron number different from the current experimental trend.

We have presented the values of the parameters used in the Hamiltonian, but have not attempted to explain their dependence on neutron number within a microscopic framework. This will be the subject of a later paper. We do, however, note once again that our results for χ_ν tend to indicate the underlying subshell structure of the 82 to 126 major shell. In particular the minimum in χ_ν at $N = 108$ may be related to a subshell closure in the $i_{13/2}$ Nilsson level.

We would also like to comment, at this point, that the global scheme for the IBA is to obtain a consistent set of parameters that will reproduce the experimental data for all even-even nuclei in a given mass region. If we compare the parameter set for the tungsten isotopes with those used for the neighboring osmium and platinum isotopes,[7] we see that they are, for the most part, consistent. Also the isotopes of xenon, barium and cerium, whose valence bosons occupy the 50–82 shell, have recently been fitted with a consistent set of parameters.[6] So we can see that the above-mentioned global scheme is being borne out by the current research. Further investigations of the isotopes of other nuclides in the $Z = 50$ to 82 and $Z \geq 82$ regions are being carried out and will be reported in a future publication.

ACKNOWLEDGMENTS

We wish to thank Professor Franco Iachello, Dr. Keith A. Sage, and Dr. Olaf Scholten for numerous useful discussions and for their continual interest in this work. We particularly thank Dr. Scholten for providing the computer codes for NPBOS and NPBEM and for helping us expand then to handle eleven bosons. We thank Dr. John Wood for providing us with recent information regarding the experimental data for the tungsten isotopes. We would like to acknowledge the partial support of this research by the National Science Foundation Grant No. PHY-7902654.

[1]A. Arima and F. Iachello, Ann. Phys. (N.Y.) 99, 253 (1976); 111, 201 (1978); O. Scholten, F. Iachello, and A. Arima, *ibid.* 115, 325 (1978).

[2]*Interacting Bosons in Nuclear Physics*, edited by F. Iachello (Plenum, New York, 1979).

[3]T. Otsuka and O. Scholten, private communication.

[4]T. Otsuka, A. Arima, F. Iachello, and I. Talmi, Phys. Lett. 76B, 139 (1978); T. Otsuka, A. Arima, and F. Iachello, Nucl. Phys. A309, 1 (1978).

[5]J. P. Schiffer and W. W. True, Rev. Mod. Phys. 48, 191 (1976).

[6]G. Puddu, O. Scholten, T. Otsuka, Nucl. Phys. A (to be published).

[7]R. Bijker, A. E. L. Dieperink, O. Scholten, and R. Spanoff, Nucl. Phys. A344, 207 (1980).

[8]M. Sakai and Y. Gono, Institute of Nuclear Study, Japan Report No. 160 (1979).

[9]L. G. Mann, J. B. Carlson, R. G. Lanier, G. L. Struble, W. M. Buckley, D. W. Heikkinen, I. D. Proctor, and R. K. Sheline, Phys. Rev. C 19, 1191 (1979).

[10]*Table of Isotopes*, 7th ed., edited by C. M. Lederer and V. S. Shirley (Wiley, New York, 1978).

[11]A. Bohr and B. Mottelson, *Nuclear Structure* (Benjamin, New York, 1969), Vol. I.

[12]W. Andrejtscheff, K. D. Schilling, and P. Manfrass, Nuclear Data Tables 16, 515 (1975).

[13]W. T. Milner, F. K. McGowan, R. L. Robinson, P. H. Stelson, and R. O. Sayer, Nucl. Phys. A177, 1 (1971).

[14]F. K. McGowan, W. T. Milner, R. O. Sayer, R. L. Robinson, and P. H. Stelson, Nucl. Phys. A289, 253 (1977).

[15]C. Günther, P. Kleinheinz, and R. F. Casten, Nucl. Phys. A172, 273 (1971).

[16]J. J. O'Brien, J. X. Saladin, C. Baktash, and B. Elbek, Nucl. Phys. A291, 510 (1977).

[17]M. J. Canty, C. Günther, P. Herzog, and B. Richter, Nucl. Phys. A203, 421 (1973).

[18]Ph. Hubert, C. Roulet, H. Sergolle, P. Colombani, J. M. Lagrange, J. Vanhorenbeeck, and N. R. Johnson, Nucl. Phys. A321, 213 (1979).

[19]A. V. Aldushchenkov and N. A. Voinova, Data Tables 11, 299 (1972).

[20]P. Russo, J. K. Sprinkle, D. Cline, A. R. Manare, and R. P. S. Scharenberg, Bull. Am. Phys. Soc. 22, 1032 (1977).

[21]J. J. O'Brien, J. X. Saladin, C. Baktash, and J. G. Alessi, Phys. Rev. Lett. 38, 324 (1977).

[22]K. Kumar and M. Baranger, Nucl. Phys. A122, 273 (1968).

[23]G. M. Kalvius and G. K. Shenoy, Nucl. Data Tables 14, 639 (1974).

[24]R. Barrett and D. Jackson, *Nuclear Sizes and Structure* (Oxford University Press, Oxford, 1977).

[25]K. Heilig and A. Steudel, Nucl. Data Tables 14, 613 (1974).

[26]R. Engfer, H. Scheuwly, J. L. Vuilleumier, H. K. Walter, and A. Zehnder, Nucl. Data Tables 14, 509 (1974).